ChemBioChem

Supporting Information

Orthogonal Peptide-Templated Labeling Elucidates Lateral ET_AR/ET_BR Proximity and Reveals Altered Downstream Signaling

Philipp Wolf, Alexander Mohr, Georgina Gavins, Victoria Behr, Karin Mörl, Oliver Seitz, and Annette G. Beck-Sickinger*

Table of content S-2

Experimental section S-3

Polymerase chain reaction primer S-3

Solid phase synthesis of the TAMRA-MPAA-GSGSG conjugate S-4

Materials S-4

Synthesis of the control conjugate S-5

Generation of nanoluciferase-arrestin-3 S-5

Inositol phosphate accumulation assay S-5

Arrestin 3 recruitment assay S-6

Statistical analysis S-6

Results S-7

Activation profile of Cys-P1/P3-ET_AR/ET_BR-GFP and proof of principle labeling S-7

Determination of orthogonal peptide-templated acyl transfer specificity S-8

Receptor activation after peptide-templated labeling S-9

Determination of labeling probe selectivity S-10

Determination of labeling efficiency S-11

GPCR interaction characteristics derived from proximity-dependent FRET S-12

Determination of ligand selectivity and GPCR activation profiles S-13

Agonist-internalization of GPCRs labeled by peptide-templated acyl transfer reaction S-14

Impact of receptor activation on internalization in co-expression setups S-15

Membrane residence time of GPCRs in the absence of agonists S-16

Selective ET_BR-mediated Ca^{2+} flux in the presence of co-transfected ET_AR S-17

Impact of GPCR co-expression on ET_BR-mediated Ca^{2+} flux in HEK293 S-19

Investigation of arrestin recruitment to activated ET_BR in co-expression setups S-21

References S-23

Experimental section

Polymerase chain reaction primer

Primer sequences used for N-terminal fusion of (SP)-Cys-P1- and (SP)-Cys-P3-tag to GPCRs and the generation of the Nluc-tagged arrestin 3 constructs are summarized in Supplementary Table S1.

Table S1: Primer sequences.

Primer		Sequence
Code	**Name**	**5'-3'**
1	Cys-P1-AT_1R fw	AAACCGATATCGCCACCATGTGCGAGATCCAGGCCCTGGAGGAGGAGAACGCCCAGCT GGAGCAGGAGAACGCCGCCCTGGAGGAGGAGATCGCCCAGCTGGAGTACGGCGGCT CAATGATTCTCAACTCTTCTACTG
2	Cys-P3-AT_1R fw	AAACCGTCGACGCCACCATGTGCGAGATCCAGCAGCTGGAGGAGGAGATCGCCCAGC TGGAGCAGAAGAACGCCGCCCTGAAGGAGAAGAACCAGGCCCTGAAGTACGGCGGCT CAATGATTCTCAACTCTTCTACTGAAGATGG
3	Cys-P1-APJ fw	AAACCGTCGACGCCACCATGTGCGAGATCCAGGCCCTGGAGGAGGAGAACGCCCAGC TGGAGCAGGAGAACGCCGCCCTGGAGGAGGAGATCGCCCAGCTGGAGTACGGCGGCT CAATGGAGGAAGGTGGTGATTTTGAC
4	Cys-P3-APJ fw	AAACCGTCGACGCCACCATGTGCGAGATCCAGCAGCTGGAGGAGGAGATCGCCCAGC TGGAGCAGAAGAACGCCGCCCTGAAGGAGAAGAACCAGGCCCTGAAGTACGGCGGCT CAATGGAGGAAGGTGGTGATTTTGAC
5	pV2-eYFP-XbaI rev	GTGGAGCCAAACGCAGTACAAAG
6	pVitro2-SalI fw	ACACAAAACGTGCAACTTGAAACTC
7	pVitro2-SalI rev	TATTGTCGACACCGGTTGCTTTGAATTAG
8	SalI-Cys-P1-AT_1R-Stop fw	AAACGTCGACACCATGTGCGAGATCCAG
9	SalI-Cys-P1/P3-GPCR-Stop fw	AAACGTCGACGCCACCATGTGCGAGATC
10	AT_1R-Stop rev	TTTGTCTAGATTACTCAACCTCAAAACATGGTGCAG
11	APJ-Stop rev	TTTGTCTAGATTAGTCAACCACAAGGGTCTCCTGGCTG
12	SP-Cys-P1-AT_1R/APJ-MP fw	AACCGGTGTCGACGCCACCATGCAGCCGCCTCCAAGTCTG
13	SP-Cys-P1-AT_1R/APJ-MP rev	CCTCCAGGGCCTGGATCTCGCATCCCCAGATCCGCGACAG
14	SP-Cys-P3-AT_1R/APJ-MP fw	AACCGGTGTCGACGCCACCATGCAGCCGCCTCCAAGTCTG
15	SP-Cys-P3-AT_1R/APJ-MP rev	CCTCCAGCTGCTGGATCTCGCATCCCCAGATCCGCGACAG
16	SP-Cys-P1-ET_AR fw	TGGCACTGGTTGGATGTGTAATCAGTTGCGAGATCCAGGCCCTG
17	SP-Cys-P1-ET_AR rev	TTGCTTAGATTTGTGCTGTATCTCTCAGGATTATCTGAGCCGCCGTACTCCAG
18	SP-Cys-P3-ET_AR fw	TGGCACTGGTTGGATGTGTAATCAGTTGCGAGATCCAGCAGCTG

19	SP-Cys-P3-ET_AR rev	TGCTTAGATTTGTGCTGTATCTCTCAGGATTATCTGAGCCGCCGTACTTCAG
20	SP-Cys-P1-ET_BR fw	CGGCCTGTCGCGGATCTGGGGATGCGAGATCCAGGCCCTG
21	SP-Cys-P1-ET_BR rev	CAGGCGGGAAGCCTCTCTCCTCTGAGCCGCCGTACTCCAG
22	SP-Cys-P3-ET_BR fw	CGGCCTGTCGCGGATCTGGGGATGCGAGATCCAGCAGCTG
23	SP-Cys-P3-ET_BR rev	CAGGCGGGAAGCCTCTCTCCTCTGAGCCGCCGTACTTCAG
24	SalI-SP-Cys-P1/3-ET_AR-Stop fw	AAACGTCGACGCCACCATGGAAACCCTTTGCCTC
25	SalI-SP-Cys-P1/3-ET_AR-Stop rev	TTTGTCTAGATTAGTTCATGCTGTCCTTATGGCTGC
26	SalI-SP-Cys-P1/3-ET_BR-Stop fw	AAACGTCGACGCCACCATGCAGCCGCCTCCAAGTC
27	SalI-SP-Cys-P1/Cys-P3-ET_BR-Stop rev	TTTGTCTAGATTAAGATGAGCTGTATTTATTACTG
28	AflII_Arr3 Fw	GACTTAAGTCTCGGCGAGCGCTCGACTCCATGGGGGAGAAACCCGGGACCAGGGTCTTC
29	Arr3 Rev	GTTGTTGAATAGGGCAAGCTTCCAGCCCTAATCGATAC
30	AsiSI_Nluc Fw	CTGGAATTCGCGATCGCGGCCACGATGGTCTTCACACTCGAAGATTTCGTTG
31	AsiSI_Nluc Rev	GAGCGCTCGCCGAGACTTAAGTCCGGACGCCAGAATGCGTTCGCACAG

Solid phase synthesis of the TAMRA-MPAA-GSGSG conjugate

Materials

N-α-Fmoc-protected amino acids, ethyl 2-cyano-2-(hydroxyimino)acetate (Oxyma), and N,N′-diisopropylcarbodiimide (DIC) were purchased from Iris Biotech (Marktredwitz, Germany). G-Wang resin and O-(7-azabenzotriazolyl)- tetramethyluronium hexafluorophosphate (HATU) were supplied from Novabiochem (Darmstadt, Germany). 6-Carboxytetramethylrhodamine (TAMRA) was purchased from ChemPep, Inc. (Wellington, Florida). Acetonitrile (ACN) was obtained from VWR (Darmstadt, Germany). Dimethylformamide (DMF) and dichloromethane (DCM) were obtained from Biosolve (Valkenswaard, The Netherlands). N,N-Diisopropylethylamine (DIPEA), 1,2-ethanedithiol (EDT), 4-methoxytriphenylmethyl chloride (Mmt-Cl), mercapto phenyl acetic acid (MPAA), piperidine, thioanisole (TA), trifluoroacetic acid (TFA), and triisopropylsilane (TIS) were purchased from Sigma-Aldrich (Taufkirchen, Germany). Diethyl ether was obtained from Merck (Darmstadt, Germany).

Synthesis of the control conjugate

S-Mmt-protected MPAA was prepared as described in the main manuscript. The control peptide was synthesized on a G-Wang resin (15 µmol scale). Automated synthesis was performed with a SYRO I peptide synthesizer (MultiSynTech; Witten, Germany), using 8 equiv. of N-α-Fmoc-protected amino acids, 8 equiv. Oxyma, and 8 equiv. DIC dissolved in DMF. Automatic coupling steps were carried out twice with a reaction time of 40 min each. For Fmoc deprotection, 40 % (v/v) piperidine in DMF was applied for 3 min and 20 % (v/v) piperidine in DMF for 10 min. The S-Mmt-MPAA-OH (4.5 equiv.) was coupled twice for 45 min each in DMF using 4.5 equiv. HATU, and 8 equiv. DIC dissolved in DMF. After Mmt deprotection, using DCM/TFA/TIS (96:2:2, 2x1 min), TAMRA was coupled with 1.9 equiv HATU and 2 equiv DIPEA for approximately 18 h at RT. Peptides were cleaved from the resin with TFA/H_2O/TIS (96:2:2) and precipitated from diethyl ether. Purification peptide was carried out on a RP-HPLC (Shimadzu) equipped with a Phenomenex Kinetex C18 100 Å column by applying a linear binary gradient of eluent A (0.1 % TFA in water, v/v) and B (0.08 % TFA in ACN). Peptide purity was confirmed by analytical RP-HPLC, and peptide identity was verified by mass spectrometry: MALDI-ToF mass spectrometry (UltraflexIII, Bruker Daltonics), and ESI-ion trap mass spectrometry (HCT, Bruker). Peptides were kept as a 10^{-4} M stock aqueous solution, containing 0.1 % TFA.

Generation of nanoluciferase-arrestin-3

The cDNA of bovine arrestin-3 (arr-3) was amplified from the previously described pcDNA3.1-Rluc3-Arr3 plasmid[1] introducing a 5' AflII restriction site (primer: 28 and 29). The Nluc cDNA, containing a 5' secretion sequence, was amplified from the pNL1.3-secLuc plasmid (kindly provided by A. Kaiser, Leipzig University) introducing a 5' AsiSI restriction site (primer: 30 and 31). The PCR products were fused by overlap extension (OE) PCR (primer: 29 and 30) and digested with AsiSI/HindIII prior to ligation into a pcDNA3.1 vector.

Inositol phosphate accumulation assay

COS-7 cells were grown in 25 cm^2 culture flasks until 70-80 % confluency was reached. Transient transfection was performed using Metafectene® Pro (according to the manufacturer's protocol) with a total of 4000 ng plasmid DNA per 25 cm^2 flask. The apelin receptor was co-transfected with the chimeric $G\alpha_{\Delta 6qi4myr}$ protein (3/1 ratio) (kindly provided by E. Kostenis (Rheinische Friedrich-Wilhelms-Universität, Bonn, Germany)).[2] After 24 h, transfected cells were seeded into 384-well plates (15,000 cells in 20 µL/well) and cultured until the experiment. Cells were stimulated with different peptide concentrations (10^{-7}-10^{-12} M) in HBSS, containing 20 mM LiCl, for 60 min at standard conditions. Cell lysis and inositol phosphate detection was performed as described by the manufacturer. Assay readout was

performed on a Tecan Spark plate reader (Tecan Group, Männedorf, Switzerland). Fluorophore emission was measured at (620/10 nm; 665/8 nm) after donor excitation (320/25 nm) and the HTRF ratio (10,000*665 $nm_{emission}$/620 $nm_{emission}$) was calculated. Concentration-response curves were generated by normalization to the respective wild type/control (bottom value = 0 %; top value = 100 %) and determination of EC_{50}/pEC_{50}, and E_{max} values was performed with the software GraphPad PRISM 5.0 (San Diego, USA).

Arrestin 3 recruitment assay

COS-7 cells were transiently transfected using Metafectene® Pro (according to the manufacturer's protocol) in 25 cm^2 cell culture flask after reaching 70 % confluency. Transfection of was performed at a 1/20 ratio of Nluc-arr3 (BRET donor) to ET_BR-GFP (BRET acceptor) plasmid DNA, balancing the total amount of plasmid DNA (4000 ng) per cell culture flask with mock DNA. One day post transfection, cells were seeded into 96-well µclear plates (100,000 cells/well) and cultured at standard conditions. All BRET experiments were performed at 37° C. The medium was replaced with BRET buffer (25 mM HEPES in HBSS, pH 7.3) and furimazine (Promega (Madison, Wisconsin)) was added (final concentration: 2.1 µM). For kinetic experiments, the baseline was monitored for 5 min before peptide addition (final concentration: 100 nM). For concentration-dependent analyses, peptides were applied in a concentration range (10^{-12} to 10^{-7} M) and the BRET signal was measured after 7.5 min. BRET studies were carried out on a Tecan Spark plate reader (Tecan Group, Männedorf, Switzerland). The luminescence was monitored from 400-440 nm and fluorophore emission was detected between 505-590 nm. The fluorescence to luminescence ratio was calculated (BRET ratio) and netBRET values were determined by subtraction of BRET signals derived from unstimulated cells. Concentration-response curves were generated by normalization to the respective wild type/control (bottom value = 0 %; top value = 100 %) and determination of EC_{50}/pEC_{50}, and E_{max} values was performed with the software GraphPad PRISM 5.0 (San Diego, USA).

Statistical analysis

Statistical analyses were performed with the software GraphPad PRISM 5.0 (San Diego, USA). Significances were calculated by one-way ANOVA and Tukey's t-test.

Results

Activation profile of Cys-P1/P3-ET_AR/ET_BR-GFP and proof of principle labeling

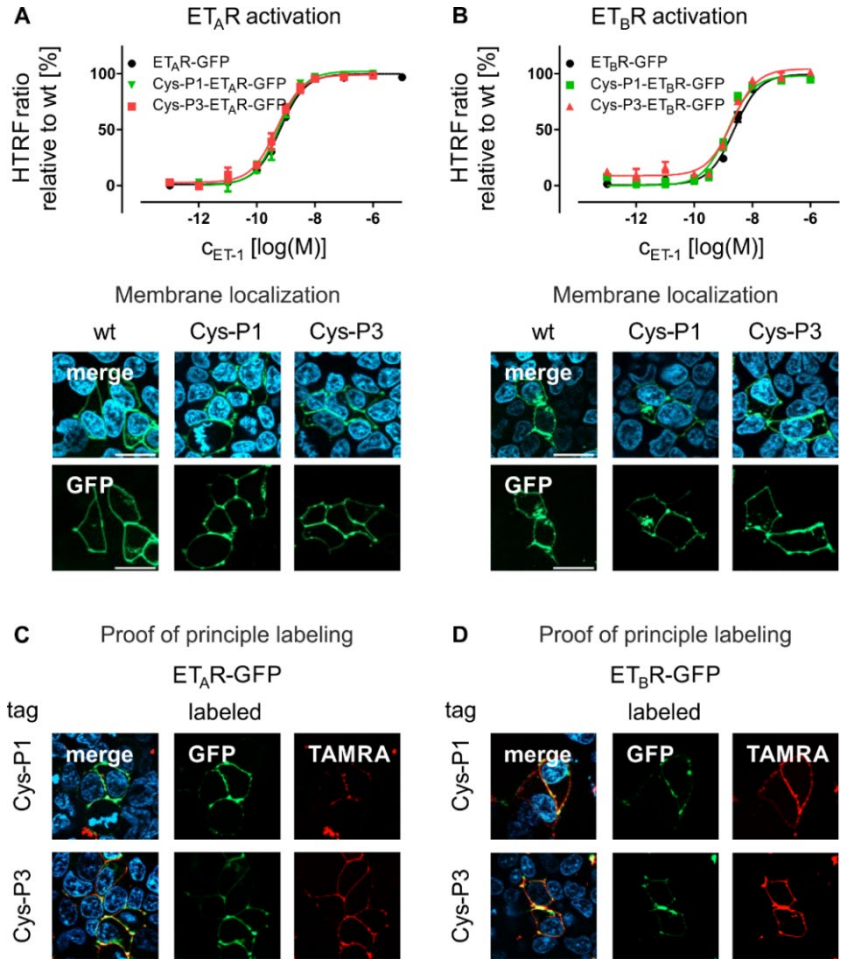

Figure S1: Activation profile of Cys-P1/P3-ET_AR/ET_BR-GFP and proof of principle labeling. GPCR activation (**A**: ET_AR; **B**: ET_BR) was investigated by inositol phosphate accumulation assay (transiently transfected COS-7 cells; n≥3 performed in triplicates). Concentration-response curves represent the mean over all assay repetitions. Membrane localization was determined in HEK293 cells either expressing wt, Cys-P1- or Cys-P3-tagged receptors (lower panels). Peptide-templated acyl transfer was carried out on Cys-P1/P3-ET_AR-GFP (**C**) or Cys-P1/P3-ET_BR-GFP (**D**) using 200 nM TAMRA-P2/-P4 in transiently transfected HEK293 cells (n≥3). Scale bar: 10 µm. Figure B is partially adapted from Gavins et al. (2021).

Table S2: Receptor activation after N-terminal modification. Activation of either wild type (wt) ET_AR/ET_BR-GFP-spark, or Cys-P1/P3-ET_AR/ET_BR-GFP was assessed in inositol phosphate accumulation assays transiently transfected COS-7 cells; n≥3 performed in triplicates).

Receptor	**ET_AR-GFP**			**ET_BR-GFP**		
Tag	**EC_{50} [nM]**	**pEC_{50} ± SEM**	**E_{max} [%] ± SEM**	**EC_{50} [nM]**	**pEC_{50} ± SEM**	**E_{max} [%] ± SEM**
wt	0.6	9.2 ± 0.03	100 ± 1	2.4	8.6 ± 0.03	99 ± 2
Cys-P1	0.6	9.2 ± 0.07	102 ± 3	1.4	8.8 ± 0.07	98 ± 3
Cys-P3	0.5	9.3 ± 0.07	99 ± 2	2.0	8.7 ± 0.09	104 ± 4

Determination of orthogonal peptide-templated acyl transfer specificity

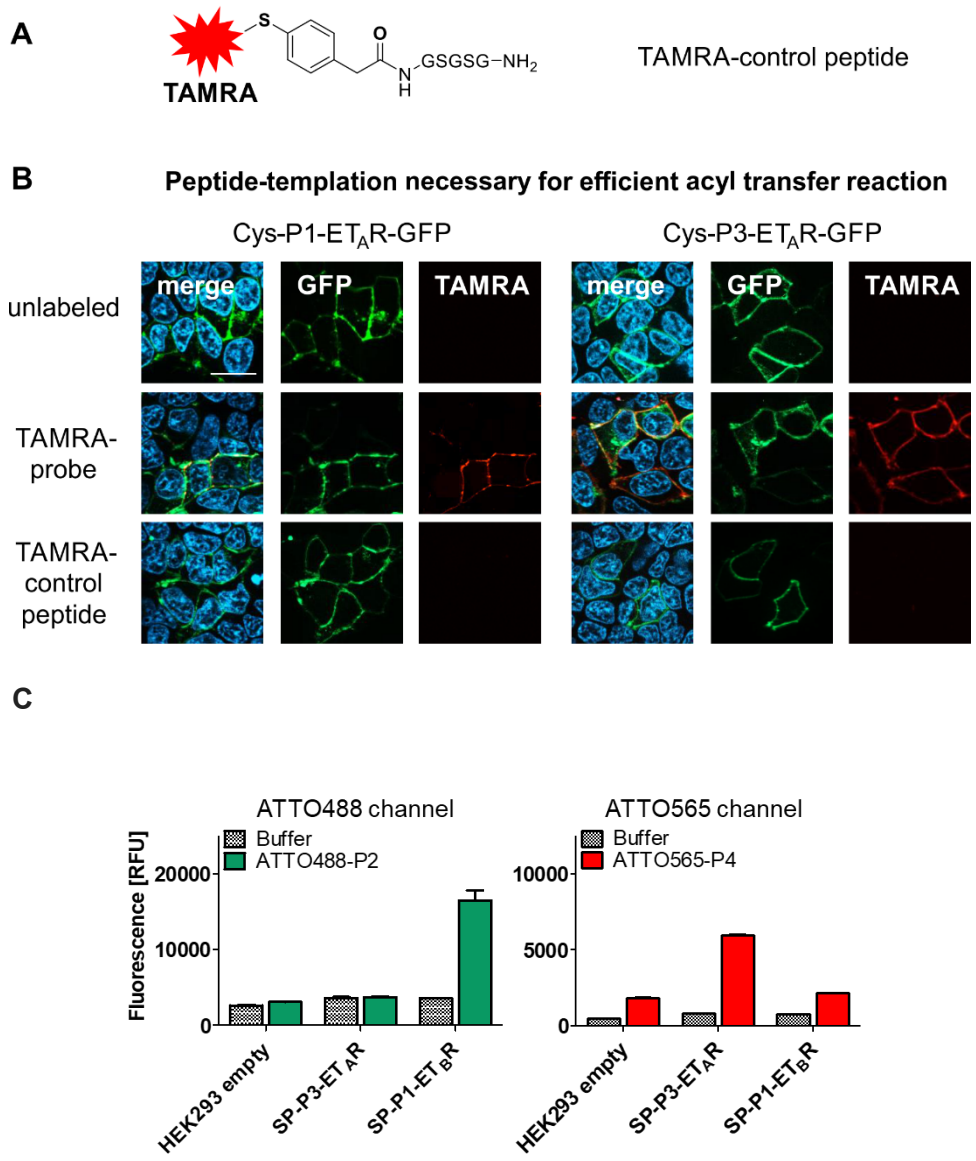

Figure S2: Determination of orthogonal peptide-templated acyl transfer specificity. (**A**) Structure of control peptide lacking the coiled-coil motif. (**B**) Peptide-templated labeling using either 200 nM 6-carboxytetramethylrhodamine (TAMRA)-control peptide, TAMRA-P2 or TAMRA-P4 on HEK293 transiently expressing either Cys-P1- or Cys-P3-ETAR-GFP (n=3). Scale bar: 10 µm. (C) Fluorescence quantification after peptide-templated labeling. Untransfected HEK293 cells or HEK293 expressing either Cys-P3-ETAR or Cys-P1-ETBR were labeled with either Atto488-P2 or Atto565-P4. After labeling, the fluorescence was measured for each condition. Successful and efficient labeling was only observed for Cys-P1/P2 and Cys-P3/P4.

Receptor activation after peptide-templated labeling

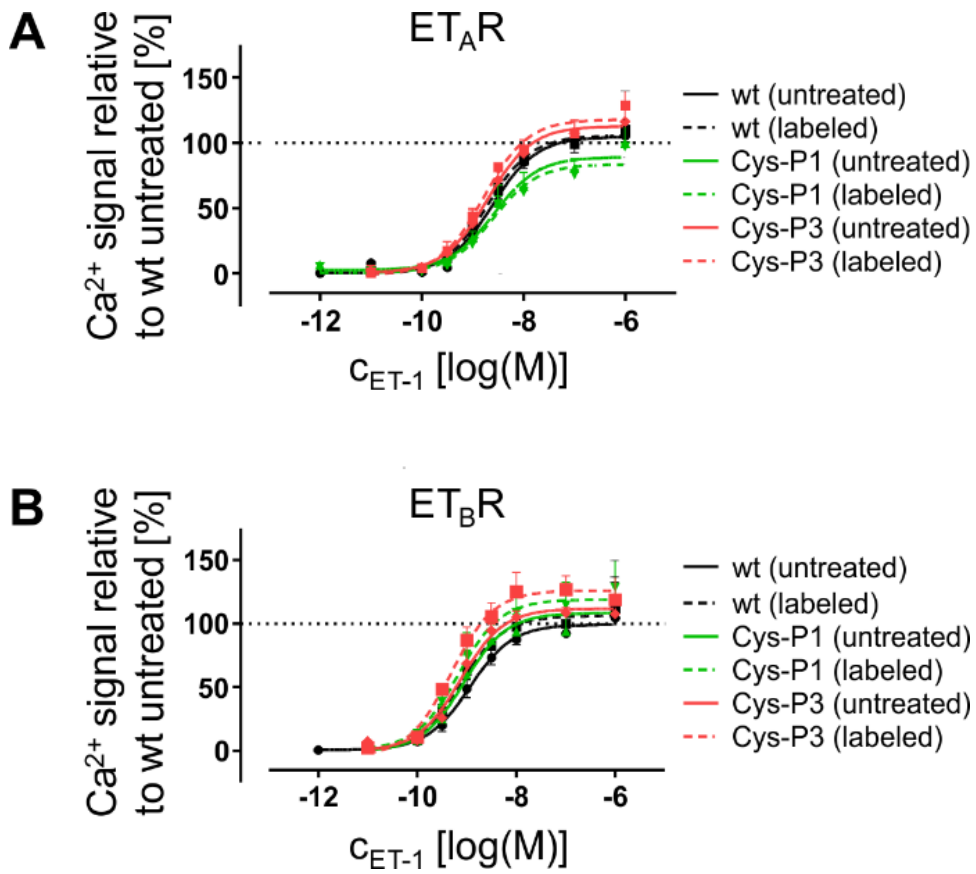

Figure S3: Receptor activation after peptide-templated labeling. (**A**) ET_AR-GFP, Cys-P1-, and Cys-P3-ET_AR-GFP or (**B**) ET_BR-GFP, Cys-P1-, and Cys-P3-ET_BR-GFP were labeled with 6-carboxytetramethylrhodamine (TAMRA)-P2 or -P4, using 0.1 mM TCEP. Agonist-triggered calcium flux was recorded after labeling (n≥3). Black: wt GPCR; green: Cys-P1-GPCR; red: Cys-P3-GPCR. Dashed lines indicate TCEP-treated cells. Signal transduction data was normalized to the wt receptors (untreated) and represent the mean over all assay repetitions.

Determination of labeling probe selectivity

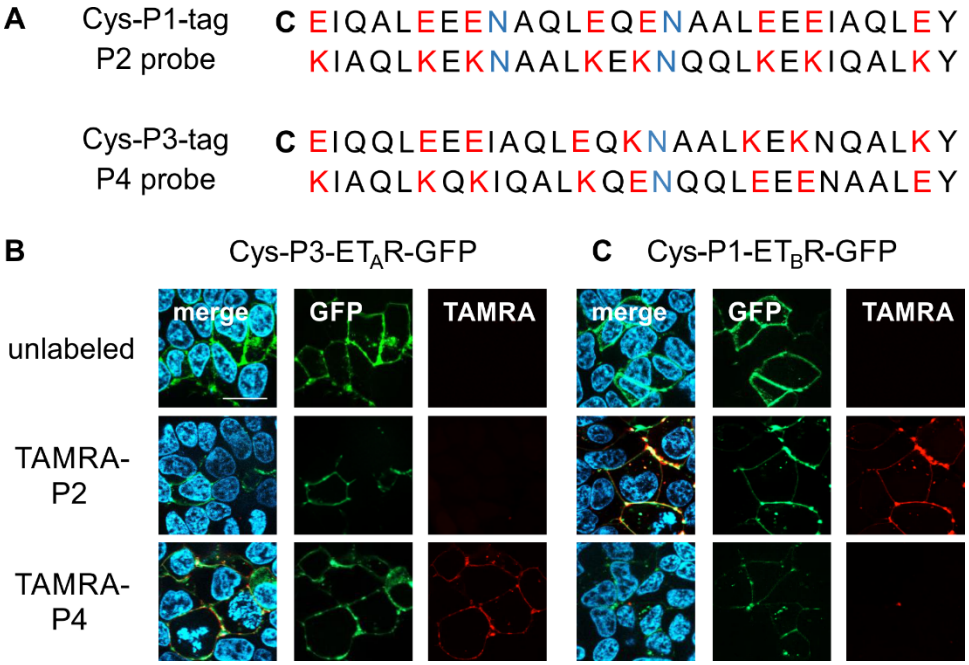

Figure S4: Determination of labeling probe selectivity. (**A**) Orthogonal coiled-coil peptide sequences (single-letter amino acid code) are depicted and interaction pattern are highlighted (hydrogen bonding: red; hydrophobic interactions: blue). Interaction specificity of the P1/P2 and P3/P4 coiled coil motifs was assessed by fluorescence microscopy by applying either 6-carboxytetramethylrhodamine (TAMRA)-P2 or TAMRA-P4 probe peptides to P3-tagged ET_AR-GFP (**B**) and P1-tagged ET_BR-GFP (**C**) expressing HEK293 cells (n=3). Scale bar: 10 µm.

Determination of labeling efficiency

A

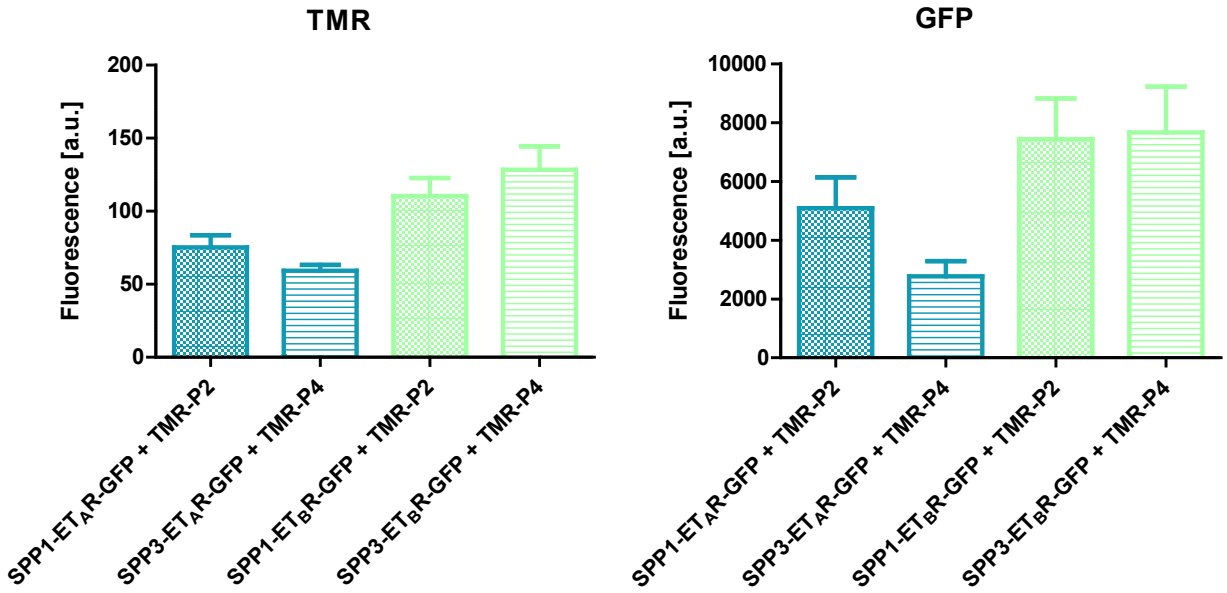

B

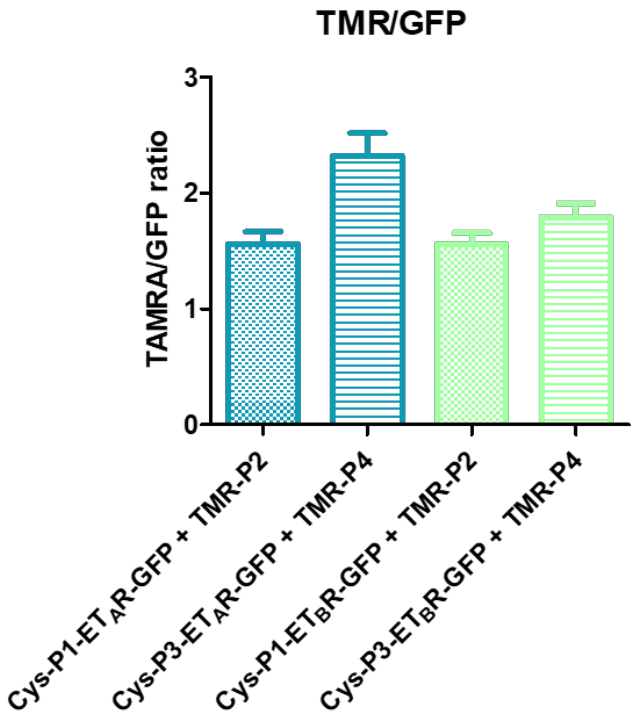

Figure S5: Determination of labeling efficiency on live cells. HEK293 cells, expressing either Cys-P1- or Cys-P3-tagged ET_AR-GFP or ET_B-GFP were labeled with TAMRA-P2 (TMR-P2) or TAMRA-P4 (TMR-P4), respectively. Total GFP and TAMRA fluorescence were measured separately (A) and the GFP/TAMRA (B) ratio was determined (n=4 in quadruplicates).

GPCR interaction characteristics derived from proximity-dependent FRET

Table S3: GPCR interaction characteristics derived from proximity-dependent FRET assays for GPCRs from different species derived from N-terminal proximity-dependent FRET assays after peptide-templated GPCR labeling in live cells. Titration experiments were performed, using constant amount of donor DNA (P1-GPCR) and adding increasing amounts of acceptor DNA (P3-GPCR) for transient transfection, which were subsequently and simultaneously labeled with Atto488-P2 (FRET donor) and Atto565-P4 (FRET acceptor). Formation of specific interaction is indicated by hyperbolic fitting (HEK293 cells, n≥2 each performed in quadruplicates).

FRET pair		**$FRET_{max}$ ± SEM**		**$FRET_{50}$ ± SEM**	**Quality of fit [R^2]**
Acceptor*	Donor*	observed[#]	regression[§]		
ET_AR	ET_AR	0.76 ± 0.09	0.96 ± 0.08	0.15 ± 0.06	0.94
ET_BR	ET_BR	0.57 ± 0.08	0.57 ± 0.05	0.25 ± 0.07	0.96
AT_1R	AT_1R	0.72 ± 0.13	0.98 ± 0.09	0.85 ± 0.17	0.97
APJ	APJ	0.58 ± 0.13	0.75 ± 0.06	0.63 ± 0.12	0.98
ET_AR	ET_BR	0.58 ± 0.09	0.65 ± 0.05	0.18 ± 0.04	0.95[a]
AT_1R	ET_AR	n.d.	n.d.	n.d.	0.92[b]
APJ	ET_AR	n.d.	n.d.	n.d.	0.99[b]
AT_1R	ET_BR	n.d.	n.d.	n.d.	0.90[b]
APJ	ET_BR	n.d.	n.d.	n.d.	0.91[b]
APJ	AT_1R	n.d.	n.d.	n.d.	0.93[b]

[a]hyperbolic fit
[b]linear fit
*acceptor construct carried the N-terminal Cys-P3-tag, whereas donor constructs were equipped with the Cys-P1-tag
[#]observed $FRET_{max}$ correlates to the experimentally determined netFRET derived from the highest A/D ratio
[§]refers to the $FRET_{max}$ value derived from the hyberbolic fit in signal saturation

Determination of ligand selectivity and GPCR activation profiles

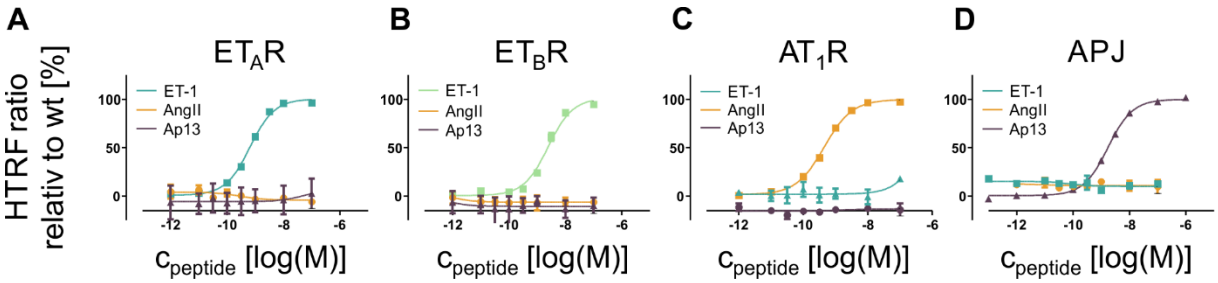

Figure S6: Determination of ligand selectivity and GPCR activation profiles. Peptide ligands AngII, Ap13 or ET-1 were administered to determine activation of ET_AR (**A**), ET_BR (**B**), AT_1R (**C**), and APJ (**D**) in inositol phosphate accumulation assays by G_q signaling (in transiently transfected COS-7 cells; n≥2 each performed in triplicates). Concentration-response curves represent the average of all assay repetitions.

Table S4: G_q activation profiles of GPCR depending on cardiovascular-active peptide ligands. Receptor activation was assessed in concentration-dependent inositol phosphate accumulation assays (in transiently transfected COS-7 cells; n≥2 each performed in triplicates). Transfected cells were stimulated either with AngII, Ap13 or ET-1. Concentration-response curves represent the average of all assay repetitions.

GPCR	Peptide ligand								
	AngII			Ap13			ET-1		
	EC_{50} [nM]	pEC_{50} ± SEM	E_{max} [%] ± SEM	EC_{50} [nM]	pEC_{50} ± SEM	E_{max} [%] ± SEM	EC_{50} [nM]	pEC_{50} ± SEM	E_{max} [%] ± SEM
ET_AR	n.d.	n.d.	n.d.	n.d.	n.d.	n.d.	0.6	9.2 ± 0.03	100 ± 1
ET_BR	n.d.	n.d.	n.d.	n.d.	n.d.	n.d.	2.4	8.6 ± 0.03	99 ± 2
AT_1R	0.4	9.3 ± 0.02	100 ± 1	n.d.	n.d.	n.d.	n.d.	n.d.	n.d.
APJ	n.d.	n.d.	n.d.	1.7	8.8 ± 0.02	100 ± 1	n.d.	n.d.	n.d.

n.d. = not detectable, Ang II - angiotensin II; AT_1R - angiotensin II receptor 1; Ap13 - apelin-13 -; APJ - apelin receptor; ET_AR - endothelin A receptor; ET_BR - endothelin B receptor; ET-1 - endothelin 1

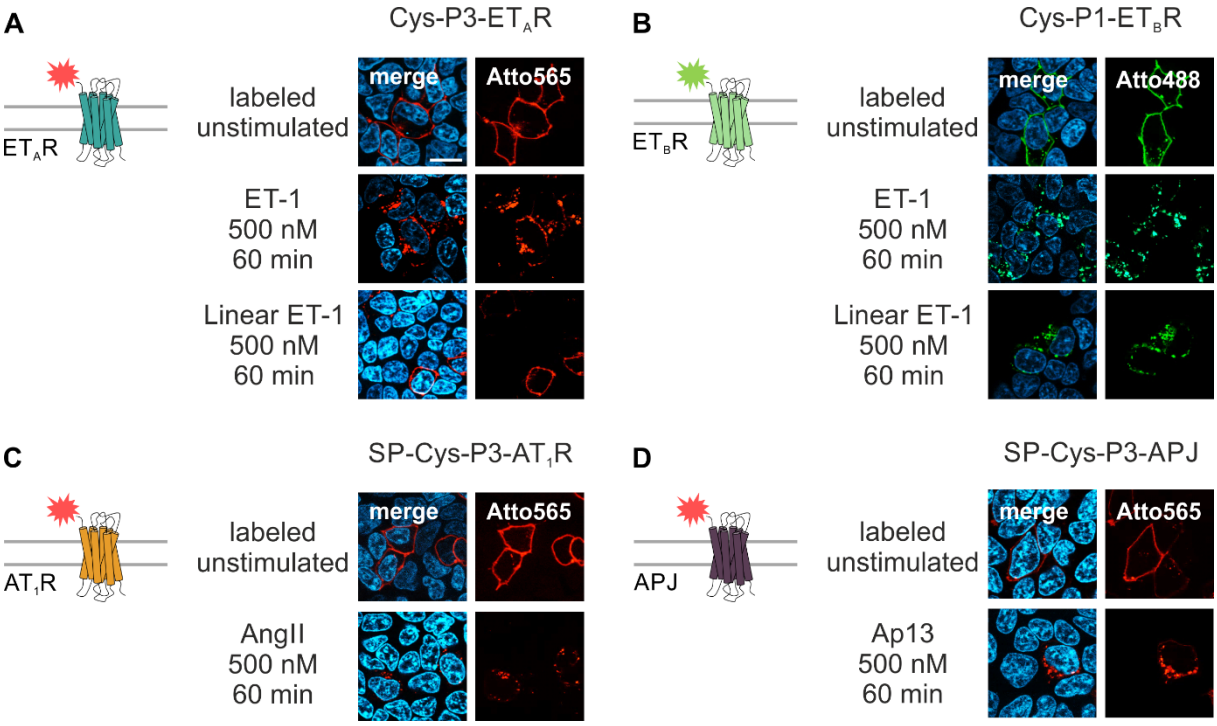

Figure S7: Agonist-internalization of GPCRs labeled by peptide-templated acyl transfer reaction in live cells. HEK293 were either transfected with Cys-P3-ET_AR (**A**), Cys-P1-ET_BR (**B**), SP-Cys-P3-AT_1R (**C**), or SP-Cys-P3-APJ (**D**). Membrane embedded GPCRs were labeled with Atto488-P2 or Atto565-P4, respectively, prior to agonist application. ET_AR- and ET_BR-expressing HEK293 cells were stimulated with either 500 nM ET-1 (dual agonist) or [$4Ala^{1,3,11,15}$,Nle^7]-ET-1 (linear ET-1, ET_BR-selective agonist) for 1 h after labeling prior to picture acquisition (n=3). For cells, expressing AT_1R or APJ, 500 nM AngII or Ap13 were applied, respectively, for 60 min after labeling prior to picture acquisition (n=3). Scale bar: 10 µm.

Impact of receptor activation on internalization in co-expression setups

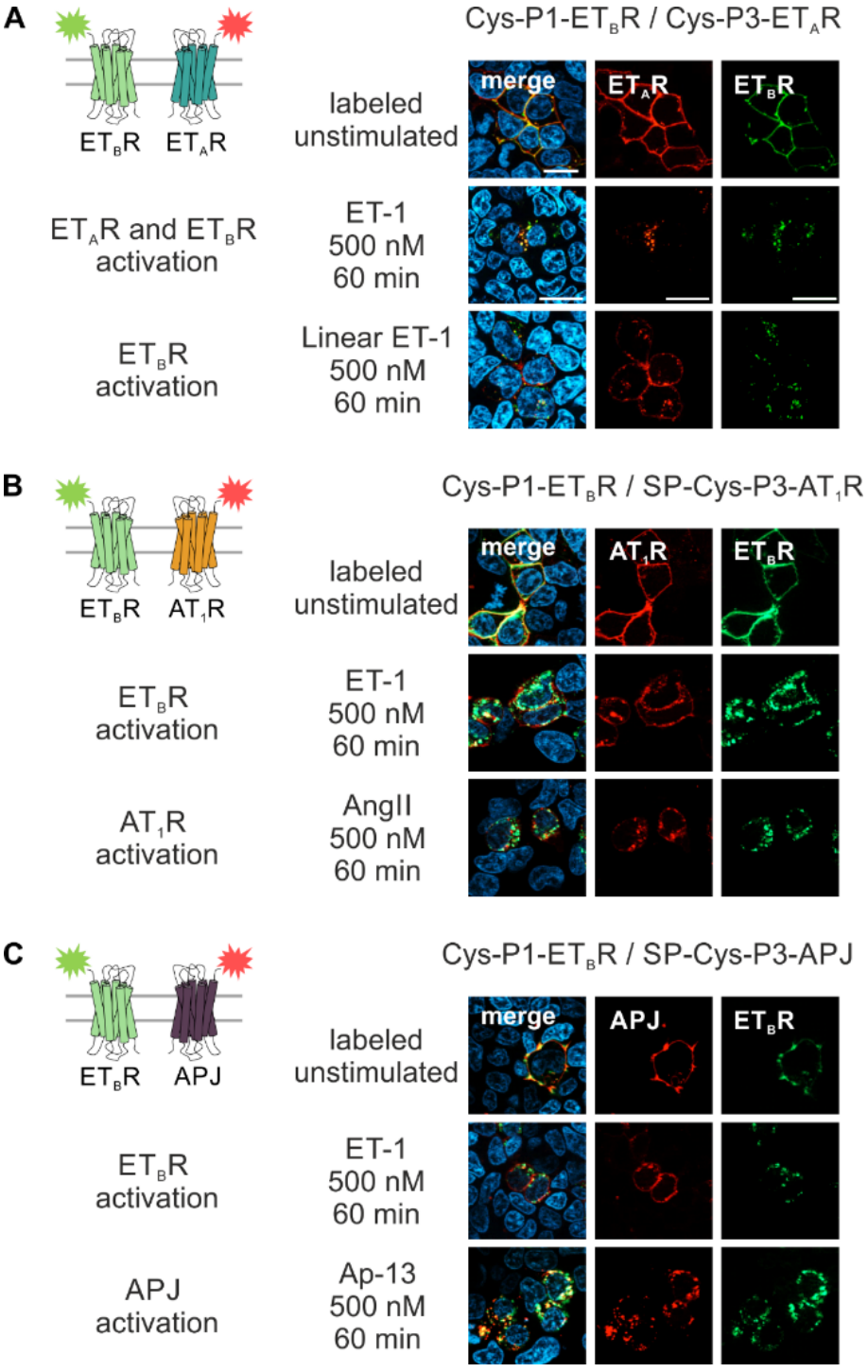

Figure S8: Impact of receptor activation on the agonist-induced internalization of the ET_BR, co-expressed with either ET_AR, AT_1R, or APJ. HEK293 were transfected with Cys-P1-ET_BR and either Cys-P3-ET_AR (**A**), SP-Cys-P3-AT_1R (**B**), or SP-Cys-P3-APJ (**C**). Membrane embedded GPCRs were labeled with Atto488-P2 (green) and Atto565-P4 (red), respectively. After peptide-templated labeling, cells were stimulated with either 500 nM ET-1 (for ET_AR or ET_BR activation), 500 nM [$4Ala^{1,3,11,15}$,Nle^{7}]-ET-1 (linear ET-1, for selective-ET_BR activation in the presence of ET_AR), 500 nM AngII (for AT_1R activation), or Ap-13 (for APJ activation) for 60 min under cell culture conditions prior to fluorescence microscopy (n≥2, representative images are shown). Scale bar: 10 µm.

Membrane residence time of GPCRs in the absence of agonists

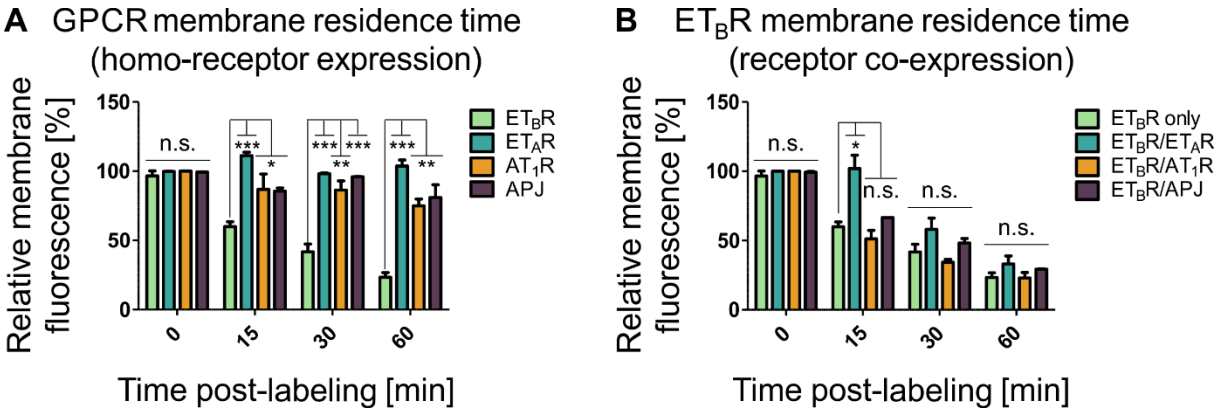

Figure S9: Membrane residence time of N-terminally labeled GPCRs in the absence of agonist administration. (**A**) Membrane-embedded Cys-P3-ET_AR, Cys-P1-ET_BR, SP-Cys-P3-AT_1R, or SP-Cys-P3-APJ were stained using the Atto488-P2 or Atto565-P4 peptide (ET_AR: blue, ET_BR: light green, AT_1R: orange, APJ: purple). (**B**) Membrane residence time of Cys-P1-ET_BR co-expressed with Cys-P3-ET_AR, SP-Cys-P3-AT_1R or SP-Cys-P3-APJ were labeled using the Atto488-P2 and Atto565-P4 peptide probe (ET_BR/mock: light green, ET_BR/ET_AR: blue, ET_BR/AT_1R: orange, ET_BR/APJ: purple). Picture acquisition was performed at distinct time point (0, 15, 30, and 60 min) post-labeling without agonist application. Membrane fluorescence was quantified for each time point and normalized to 0 min (100 %) and background fluorescence (0 %). Quantitative data represent the average over all assay repetitions (n≥2 with 10-15 cells analyzed per time point and experiment). Significance was determined by one-way ANOVA and Tukey's post test, n.s.: not significant, **: P<0.01; ***: P<0.001). Scale bar: 10 µm.

Selective ET_BR-mediated Ca^{2+} flux in the presence of co-transfected ET_AR

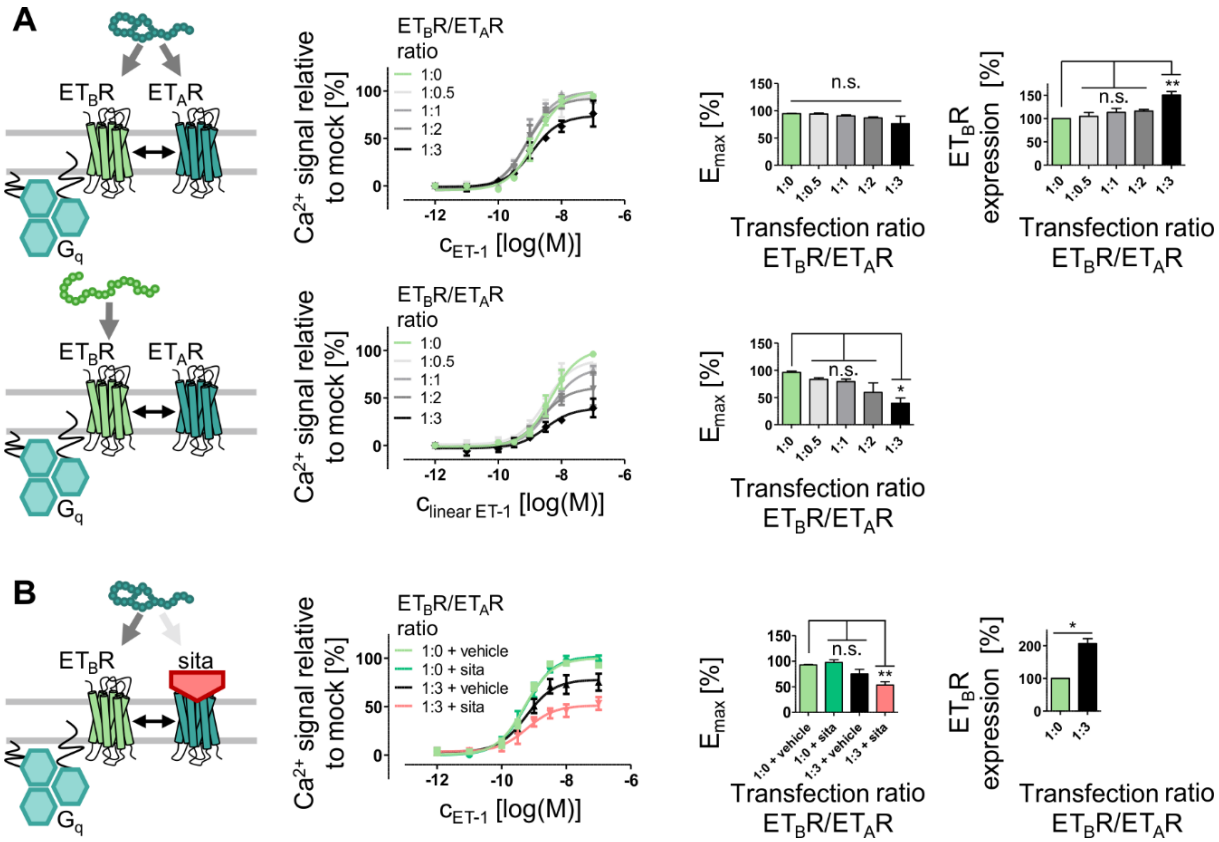

Figure S10: Selective ET_BR-mediated Ca^{2+} flux in the presence of co-transfected ET_AR. COS-7 cells were transiently transfected with constant amounts of ET_BR-GFP increasing amounts of Cys-P3-ET_AR in a ratio range from 1:0 to 1:3. Cells, expressing both ET_AR and ET_BR were stimulated with the ET_AR/ET_BR dual agonist ET-1 (**A**) or the ET_BR-selective [4Ala^{1,3,11,15}, Nle^{7}]-ET-1 (linear ET-1). The ET_AR-selective antagonist sitaxentan (red symbol, sita) was applied for selective ET_BR activation by ET-1 in the presence of co-expressed ET_AR (**C**). ET_BR-GFP expression was monitored by GFP fluorescence. Ca^{2+} flux mediated by Gq protein (turquoise) activation was monitored in COS-7 cells in duplicates and concentration-response curved represent the average over all assay repetitions (n=3; significance was determined by one-way ANOVA and Tukey's post test, n.s.: not significant, *: P<0.05, **: P<0.01).

Table S5: Selective ET_BR-mediated Ca^{2+} flux in the presence of co-transfected ET_AR. COS-7 cells were transiently transfected with constant amounts of ET_BR-GFP increasing amounts of Cys-P3-ET_AR in a ratio range from 1:0 to 1:3. Cells, expressing both ET_AR and ET_BR were stimulated with the ET_AR/ET_BR dual agonist ET-1 or the ET_BR-selective [$4Ala^{1,3,11,15}$, Nle^7]-ET-1. ET_BR-GFP expression was monitored by GFP fluorescence. Ca^{2+} flux was monitored in COS-7 cells in duplicates and concentration-response curved represent the average over all assay repetitions (n=3).

Co-transfection ratio		Relative Ca^{2+} flux initiated by ET_BR-GFP						
		ET_BR expression	ET-1			Linear ET-1		
		[%] ± SEM	EC_{50} [nM]	pEC_{50} ± SEM	E_{max} [%] ± SEM	EC_{50} [nM]	pEC_{50} ± SEM	E_{max} [%] ± SEM
ET_BR/ ET_AR	1:0	100 ± 1	1.5	8.8 ± 0.09	100 ± 5	4.7	8.3 ± 0.09	103 ± 6
	1:0.5	105 ± 8	0.9	9.0 ±0.15	96 ± 7	3.1	8.5 ± 0.10	90 ± 5
	1:1	113 ± 8	0.9	9.1 ± 0.12	99 ± 5	4.5	8.3 ± 0.08	81 ± 4
	1:2	116 ± 3	0.8	9.1 ± 0.10	93 ±4	2.4	8.6 ± 0.18	61 ± 6
	1:3	150 ± 8	1.2	8.9 ± 0.14	74 ± 5	3.1	8.5 ± 0.19	39 ± 5

Table S6: Selective ET_BR-mediated Ca^{2+} flux in the presence of co-transfected ET_AR. COS-7 cells were transiently transfected with constant amounts of ET_BR-GFP and a 3-fold excess of Cys-P3-ET_AR. Cells, expressing both ET_AR and ET_BR were stimulated with the ET_AR/ET_BR dual agonist ET-1 in the absence and presence of the ET_AR-selective antagonist sitaxentan or DMSO (vehicle control). ET_BR-GFP expression was monitored by GFP fluorescence. Ca^{2+} flux was monitored in COS-7 cells in duplicates and concentration-response curved represent the average over all assay repetitions (n=3).

Co-transfection ratio		Relative Ca^{2+} flux initiated by ET_BR-GFP						
		ET_BR expression	ET-1 + vehicle (DMSO)			ET-1 + 500 nM Sitaxentan		
		[%] ± SEM	EC_{50} [nM]	pEC_{50} ± SEM	E_{max} [%] ± SEM	EC_{50} [nM]	pEC_{50} ± SEM	E_{max} [%] ± SEM
ET_BR/ ET_AR	1:0	100 ± 1	0.5	9.3 ± 0.07	100 ±3	0.6	9.3 ± 0.09	102 ± 4
	1:3	206 ± 15	0.6	9.2 ± 0.13	88 ± 4	0.6	9.2 ± 0.18	51 ± 4

Impact of GPCR co-expression on ET_BR-mediated Ca^{2+} flux in HEK293

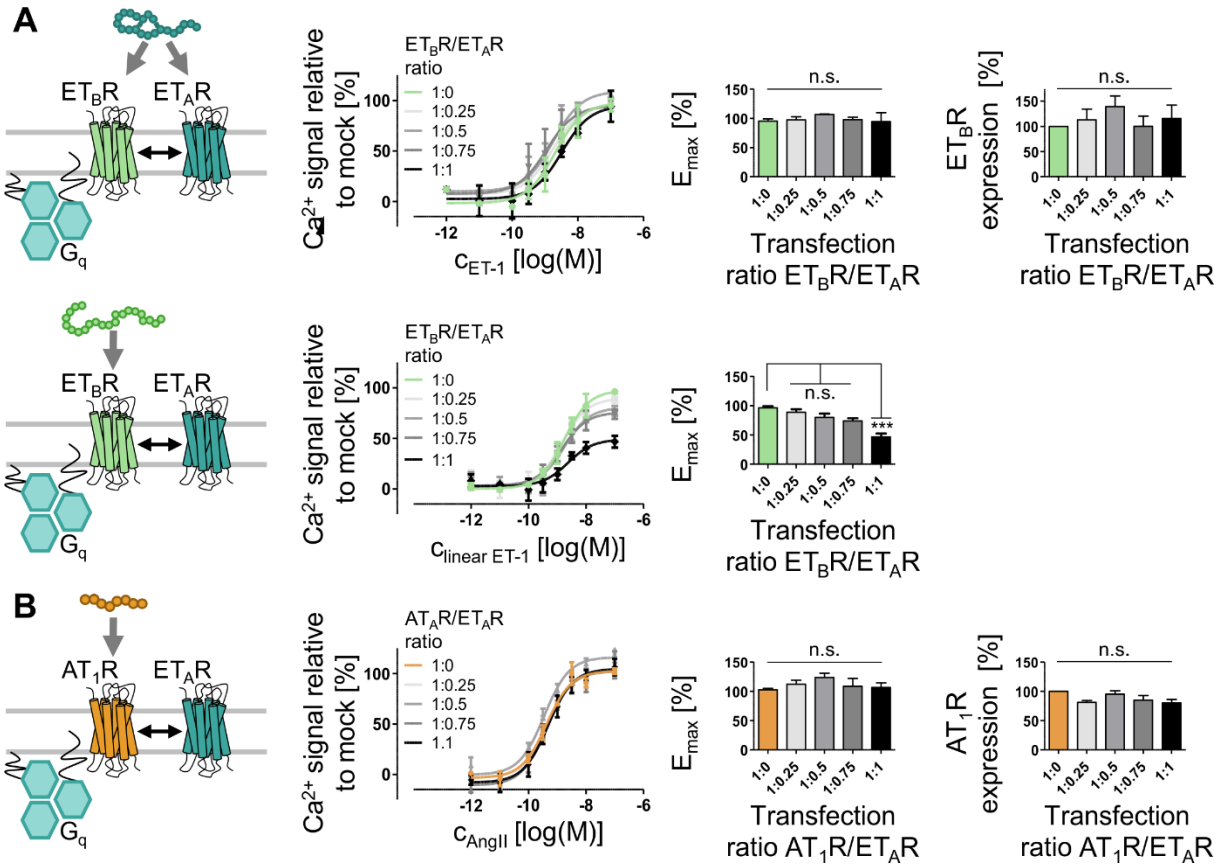

Figure S11: Impact of GPCR co-expression on ET_BR-mediated Ca^{2+} flux in HEK293 cells. (**A**) Constant amounts of ET_BR-GFP were co-transfected with increasing amounts of Cys-P3-ET_AR in a ratio range from 1:0 to 1:1. Cells, expressing both ET_AR and ET_BR were stimulated with the ET_AR/ET_BR dual agonist ET-1 (upper row) or the ET_BR-selective [$4Ala^{1,3,11,15}$, Nle^{7}]-ET-1 (lower row). ET_BR-GFP expression was monitored by GFP fluorescence. (**B**) To validate the specific effect, constant amounts of AT_1R-YFP were co-transfected with increasing amounts of Cys-P3-ET_AR in a ratio range from 1:0 to 1:1 and cells AngII for AT_1R activation. AT_1R-YFP expression was monitored by YFP fluorescence. Ca^{2+} flux mediated by Gq protein (turquoise) activation was monitored in HEK293 cells in duplicates and concentration-response curved represent the average over all assay repetitions (n=3; significance was determined by one-way ANOVA and Tukey's post test, n.s.: not significant, ***: $P < 0.001$.

Table S7: Characterization of ET_BR signaling in transiently transfected HEK293 cells. Constant amounts of ET_BR-GFP were co-transfected with increasing amounts of Cys-P3-ET_AR. Cells, expressing both ET_AR and ET_BR were stimulated with the ET_AR/ET_BR dual agonist ET-1, the ET_BR-selective [4Ala^{1,3,11,15}, Nle^{7}]-ET-1. ET_BR-GFP expression was monitored by GFP fluorescence. Ca^{2+} flux was monitored in HEK293 cells in duplicates and concentration-response curved represent the average over all assay repetitions (n=3).

Co-transfection ratio		Relative Ca^{2+} flux initiated by ET_BR-GFP						
		ET_BR expression	ET-1			Linear ET-1		
		[%] ± SEM	EC_{50} [nM]	pEC_{50} ± SEM	E_{max} [%] ± SEM	EC_{50} [nM]	pEC_{50} ± SEM	E_{max} [%] ± SEM
ET_BR/ ET_AR	1:0	100 ± 1	2.0	8.7 ± 0.12	100 ± 6	1.7	8.8 ± 0.10	98 ± 5
	1:0.25	112 ± 21	1.8	8.8 ± 0.11	98 ± 5	1.5	8.8 ± 0.13	90 ± 6
	1:0.5	139 ± 21	1.8	8.8 ± 0.18	109 ± 9	1.7	8.8 ± 0.17	80 ± 6
	1:0.75	100 ± 20	1.1	9.0 ± 0.27	95 ± 11	1.4	8.8 ± 0.15.	76 ± 5
	1:2	116 ± 27	3.2	8.5 ± 0.21	95 ± 11	2.4	8.6 ± 0.24	49 ± 6

Table S8: Characterization of AT_1R signaling in transiently transfected HEK293 cells. Constant amounts of AT_1R-YFP were co-transfected with increasing amounts of Cys-P3-AT_1R. Cells, expressing both receptors were stimulated with the AngII for selective AT_1R activation. AT_1R-YFP expression was monitored by YFP fluorescence. Ca^{2+} flux was monitored in HEK293 cells in duplicates and concentration-response curved represent the average over all assay repetitions (n=3).

Co-transfection ratio		Relative Ca^{2+} flux initiated by AT_1R-YFP			
		AT_1R expression	AngII		
		[%] ± SEM	EC_{50} [nM]	pEC_{50} ± SEM	E_{max} [%] ± SEM
AT_1R/ ET_AR	1:0	100 ± 1	0.4	9.4 ± 0.10	103 ± 4
	1:0.25	81 ± 3	0.5	9.3 ± 0.11	103 ± 5
	1:0.5	95 ± 6	0.3	9.5 ± 0.10	116 ± 4
	1:0.75	85 ± 8	0.4	9.4 ± 0.12	102 ± 5
	1:2	81 ± 5	0.5	9.3 ± 0.12	105 ± 5

Arrestin recruitment to activated ET_BR in co-expression setups

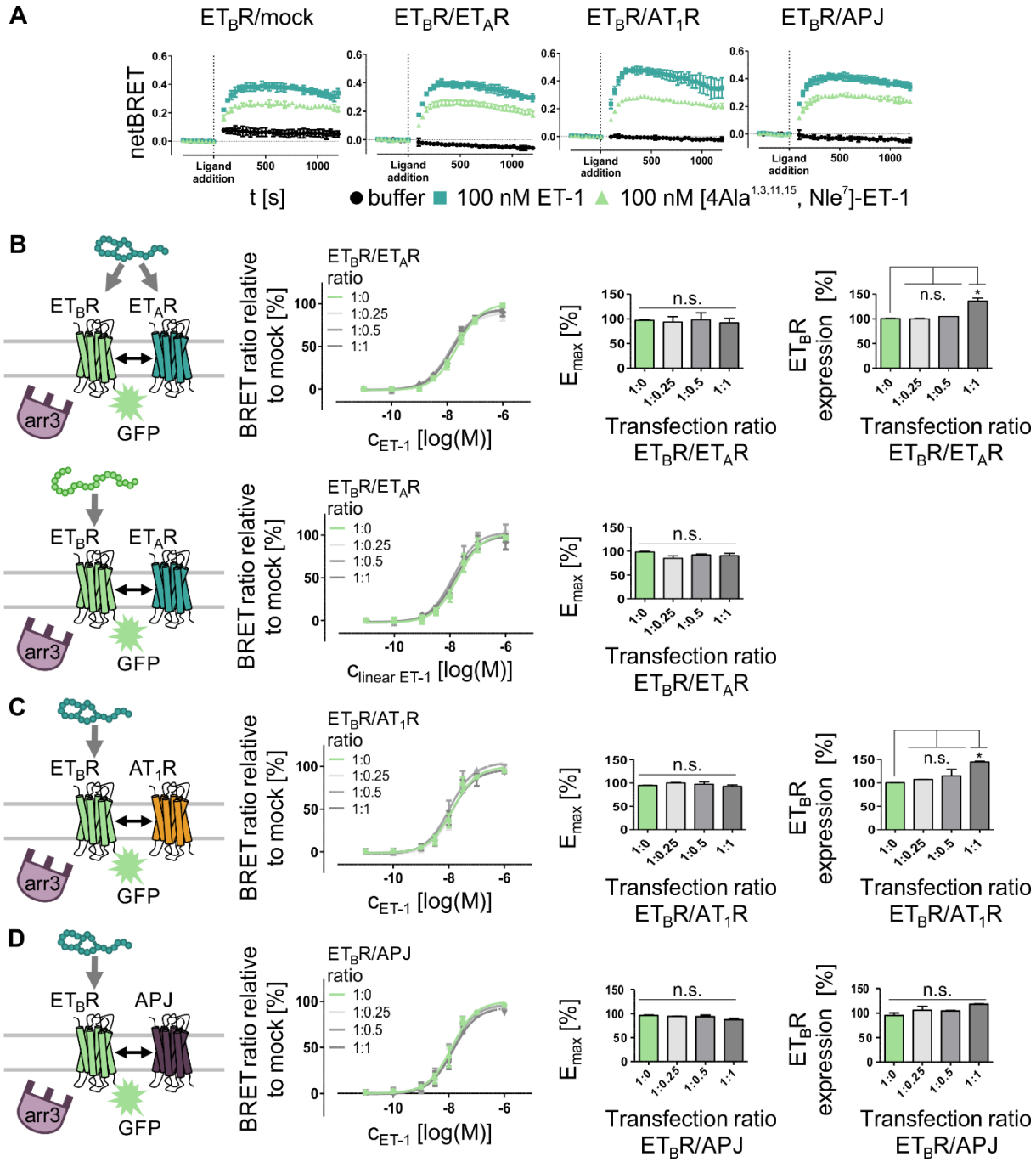

Figure S12: Investigation of arrestin recruitment to activated ET_BR in the presence of co-expressed GPCRs. (**A**) For kinetic studies of arr3 recruitment, COS-7 cells were transiently transfected with constant amounts of ET_BR-GFP and increasing amounts of Cys-P3-tagged ET_AR, AT_1R or APJ (left to right). The recruitment was monitored for 5 min (basal, light grey) before ligand addition and 15 min after addition of ET-1 (black) or linear ET-1 (dark grey). Kinetic analyses were performed in quadruplicates (n=3) and one representative kinetic trace is shown. Concentration-dependent investigation of arr3 (purple) recruitment to ET_BR-GFP in the presence Cys-P3-ET_AR (**B/C**), SP-Cys-P3-AT_1R (**E**) or SP-Cys-P3-APJ (**F**). Transfected cells were stimulated with ET-1 (**B**, **E**, **F**) or the ET_BR-selective [4Ala^{1,3,11,15}, Nle^7]-ET-1 (**C**). ET_BR expression was monitored by total GFP fluorescence. Arr3 recruitment was investigated in triplicates and concentration-response curves represent the average of all assay repetitions (n=3). Significance was determined by one-way ANOVA and Tukey's post test, n.s.: not significant, *: P<0.05). Scale bar: 10 µm.

Table S9: Characterization of arr3 recruitment to ET_BR-GFP was assessed by concentration-dependent analyses in the presence Cys-P3-ET_AR, SP-Cys-P3-AT_1R, or SP-Cys-P3-APJ. Transfected COS-7 cells were stimulated with ET-1 or the ET_BR-selective [4Ala^{1,3,11,15}, Nle^7]-ET-1 (linear ET-1). ET_BR expression was monitored by total GFP fluorescence. Arr3 recruitment was investigated in triplicates and concentration-response curves represent the average of all assay repetitions (n=3).

Co-transfection ratio		Arrestin 3 recruitment to ET_BR-GFP						
		ET_BR expression	ET-1			Linear ET-1		
		[%] ± SEM	EC_{50} [nM]	pEC_{50} ± SEM	E_{max} [%] ± SEM	EC_{50} [nM]	pEC_{50} ± SEM	E_{max} [%] ± SEM
ET_BR/ ET_AR	1:0	100 ± 1	19	7.7 ± 0.9	102 ± 5	23	7.6 ± 0.06	100 ± 3
	1:0.25	100 ± 1	16	7.8 ± 0.10	100 ± 5	14	7.8 ± 0.05	91 ± 2
	1:0.5	105 ± 1	13	7.9 ± 0.11	104 ± 5	14	7.9 ± 0.05	94 ± 2
	1:1	136 ± 6	15	7.8 ± 0.09	99 ± 4	15	7.8 ± 0.06	94 ± 6
ET_BR/ AT_1R	1:0	100 ±1	13	7.9 ± 0.09	100 ± 4	n.d.	n.d.	n.d.
	1:0.25	107 ± 1	16	7.8 ± 0.07	106 ± 4	n.d.	n.d.	n.d.
	1:0.5	115 ±14	11	8.0 ± 0.10	104 ± 5	n.d.	n.d.	n.d.
	1:1	144 ± 2	13	7.9 ± 0.09	98 ± 0.09	n.d.	n.d.	n.d.
ET_BR/ APJ	1:0	95 ± 5	13	7.9 ± 0.08	100 ± 4	n.d.	n.d.	n.d.
	1:0.25	105 ± 8	14	7.9 ± 0.09	98 ± 4	n.d.	n.d.	n.d.
	1:0.5	104 ± 1	12	7.9 ± 0.10	97 ± 5	n.d.	n.d.	n.d.
	1:1	118 ± 1	14	7.9 ±0.09	94 ± 4	n.d.	n.d.	n.d.

n.d. = not determined

References

[1] S. A. Vishnivetskiy, L. E. Gimenez, D. F. Francis, S. M. Hanson, W. L. Hubbell et al., *J. Biol. Chem.* **2011** *286*, 24288-24299.

[2] E. Kostenis, *J. Recept. Signal Transduct. Res.* **2002**, *22*, 267-281.